# General Disclaimer

## One or more of the Following Statements may affect this Document

- This document has been reproduced from the best copy furnished by the organizational source. It is being released in the interest of making available as much information as possible.

- This document may contain data, which exceeds the sheet parameters. It was furnished in this condition by the organizational source and is the best copy available.

- This document may contain tone-on-tone or color graphs, charts and/or pictures, which have been reproduced in black and white.

- This document is paginated as submitted by the original source.

- Portions of this document are not fully legible due to the historical nature of some of the material. However, it is the best reproduction available from the original submission.

Produced by the NASA Center for Aerospace Information (CASI)

# Experiments on the Large-Scale Structure of Turbulence in the Near-Jet Region

M. A. Badri Narayanan and Donald M. Kuehn

April 1979

# Experiments on the Large-Scale Structure of Turbulence in the Near-Jet Region

M. A. Badri Narayanan
Donald M. Kuehn, Ames Research Center, Moffett Field, California

# NOMENCLATURE

D       diameter of the jet at the nozzle exit

f       frequency, $\dfrac{N_c}{2}$

$N_c$       zero crossings per second

$R_D$       Reynolds number, $\dfrac{U_e D}{\nu}$

$S_t$       Strouhal number, $\dfrac{fD}{U}$

U       mean velocity

$U_e$       mean velocity at the nozzle exit, on the centerline

$U_o$       mean velocity at the centerline of the jet at any x station

u'       fluctuating velocity in the x direction

v'       fluctuating velocity in the y direction

$\overline{(u'v')}_c$       one component of the total $\overline{u'v'}$ in the four-quadrant analysis

$\tilde{u}$       RMS of u', $\sqrt{\overline{u'^2}}$

$\tilde{v}$       RMS of v', $\sqrt{\overline{v'^2}}$

t       time during which the positive spikes persist in the u'v' trace (fig. 13)

$T_{u'}$       period of the zero crossing frequency for u' (fig. 13)

$T_{u'v'}$       time interval between adjacent, positive spikes in the u'v' trace (fig. 13)

x       coordinate in the direction of the flow measured from the nozzle exit

y       coordinate perpendicular to the flow measured from the centerline of the jet

$\alpha$       half of the total jet-spreading angle

$\delta$       half width of the jet

# EXPERIMENTS ON THE LARGE-SCALE STRUCTURE OF TURBULENCE

## IN THE NEAR-JET REGION

M. A. Badri Narayanan and Donald M. Kuehn

Ames Research Center

## SUMMARY

The near region of an axisymmetric, turbulent jet was investigated. Turbulence quantities, as well as mean velocities, were measured between 3 and 23 diam away from the nozzle. The mean velocity profiles were similar over most of this distance, whereas the turbulence quantities were far from equilibrium conditions. Across the jet, the rate of large-scale turbulence varied considerably; however, a Strouhal number based on local velocity, the diameter of the jet, and the frequency of the large-scale turbulent oscillation remained relatively constant. The formation of the initial instability waves and the pairing of the vortices were examined. Turbulent fluctuations were observed only downstream of the pairing process.

## INTRODUCTION

A study of the structure of turbulence in the near-jet region has gained importance in recent years because of speculation about the relationship between large-scale velocity fluctuations and the noise production. Experiments with laboratory jets have indicated that the noise produced by the jet has a spectral peak at a Strouhal number ($fD/U_e$) of about 0.3 (refs. 1 and 2), where $D$ is the diameter of the nozzle, f is the peak frequency, and $U_e$ is the velocity at the nozzle exit. Investigations on the noise radiated by the jet engine exhausts (refs. 3 and 4) have also shown that maximum intensity occurs at the same Strouhal number (about 0.3) in the near field as well as in the far field. Fuchs has attributed this result to the turbulent fluctuations traveling downstream in a deterministic wave-like manner.

Another interesting feature of the axisymmetric jet is the formation of vortex rings. The core flow ejected through the nozzle, together with the outer flow entrained by the jet, produce vortex rings. These rings travel downstream at different speeds and merge at some distance from the nozzle exit where considerable interaction between the two flow fields occurs. It is speculated (ref. 5) that this interaction, more generally known as the pairing process, produces large local pressure fluctuations. A portion of this fluctuation is radiated as noise into the ambient air surrounding the flow. The pairing process is associated with transition in the jet from laminar to turbulent, and seems to influence the formation of the large-scale structure of turbulence for many diameters downstream.

The purpose of the present investigation was to describe some of the basic features of the near-field jet flow as they relate to the formation of the large-scale turbulent structure. Time-averaged velocities and some turbulence quantities were measured. In addition, observations were made of the formation of unstable waves and vortex pairing. Although the latter measurements were not greatly detailed, certain characteristics of the flow structure were revealed.

## EXPERIMENTS

The experiments were conducted in an axisymmetric air jet. A short nozzle ($D = 12.7$ mm) with a large contraction ratio was employed to have laminar flow at the exit. The jet was operated from a dust-free, dry-air reservoir. A large settling chamber containing flow straighteners and sound absorption material was incorporated between the pressure source and the nozzle, with a control valve in series. The maximum exit velocity on the centerline was 54.6 m/sec with the valve fully open. A sketch of the experimental setup is shown in figure 1.

Measurements within the jet were made with a pitot tube and with hot wire probes. The mean velocity profiles were determined from pressure measurements using a small pitot tube (0.5 mm diam) and a sensitive pressure transducer. Ambient pressure surrounding the jet was used as the static pressure for the evaluation of the mean velocity. A single, normal hot wire was also used to measure mean velocity. Fluctuating velocities were measured with the single-wire probe and with a cross-wire probe. The wires ($P_t - R_h$) were 5 $\mu_m$ in diameter and 1 mm long. They were operated by a constant temperature DISA anemometer. Instantaneous $u'$, $v'$, and $u'v'$ signals were obtained simultaneously with adding, subtracting, and multiplying circuits. Duplicate measurements of mean velocity (pitot tube and normal wire), and fluctuating velocity in the x-direction (normal wire and cross wire) were made to evaluate the accuracy of instrumentation and technique. Measurements by different techniques agreed within the scatter of the measurements by a single instrument. The electronic system had a cut-off frequency of 1 Hz at the low end and 10 kHz at the high end. A schematic diagram of the circuit arrangement is shown in figure 2. The output signals ($u'$,$v'$,$u'v'$) from the electronic processors were recorded on an FM tape recorder at a tape speed of nearly 3 m/sec. Some of these data were later retraced on a Beckman strip-chart pen recorder. The play-back speed was 1/64 of the original speed. Because the frequency response of the recorder was flat up to 100 Hz, velocity fluctuations up to 6400 Hz could easily be traced. These traces were used for examining certain features of the instantaneous fluctuations.

## RESULTS AND DISCUSSION

The investigation was divided into two parts. For the first set of experiments, we measured the mean velocity profiles and the intensity of the velocity fluctuations at four stations downstream of the nozzle, namely x/D of 3.3,

2

6.7, 11.9, and 22.8. The first station was near the end of the potential core region where the mean velocity along the centerline of the jet remained constant. These results were confined to a single exit velocity ($U_e$) of 54.6 m/sec; the corresponding Reynolds number ($U_e D/\nu$) was approximately 45000. The second set of experiments focused on the formation of the periodic disturbances in the vicinity of the nozzle exit and on the large-scale turbulent fluctuations. A qualitative study of the pairing process was made.

## Mean-flow Measurements

The mean-flow velocity data are shown in figures 3–7. The measured velocity profiles are shown in figure 3. In this plot, velocity has been nondimensionalized by $U_0$ to separate the curves for clarity. The value of $U_0$ was easily and accurately determined. However, the distance normal to the jet centerline has not yet been normalized because the value of $\delta$ is arbitrary and more difficult to determine than $U_0$. In addition, it will be shown that the choice of $\delta$ is important because the resulting data correlations are altered appreciably by the choice of a value for $\delta$.

Boundary-layer thickness (or jet thickness) is defined as the distance from the centerline to the point where the mean velocity is a chosen percentage of $U_0$. Initially, $\delta$ was chosen at $0.05U_0$. This variation of $\delta$ with $x/D$ is shown in figure 4, and the nondimensional mean-flow velocity profiles are shown in figure 5. The value of $\delta$ at $0.05U_0$ shows considerable scatter primarily a result of the fact that (1) the velocities at the edge of the jet approach zero so gradually and (2) these very small velocities are difficult to measure accurately. For the data in figure 5, we used $\delta$ determined at $0.05U_0$; these velocity profiles are not similar.

To avoid the problem of choosing a value of $\delta$ where the velocity gradient is so small, values of $\delta$ were also determined at $0.1U_0$ and $0.2U_0$. Only the data at $0.05U_0$ and $0.1U_0$ are shown because no significant change occurred by going from $0.1U_0$ to $0.2U_0$. Figure 4 shows that the scatter of $\delta$ has been considerably reduced by taking $\delta$ at $0.1U_0$. In either case, the total spreading angle of the jet is approximately $30°$. The improved accuracy of $\delta$ however, becomes most apparent where $\delta$ is used to nondimensionalize distance (e.g., compare figs. 5 and 6). The character of the data changed remarkably. As expected, similarity would not be achieved close to the nozzle exit (e.g., at $x/D = 3.3$), but the velocity profiles now show similarity beginning about 6D downstream.

Data for low-speed jets generally exist only for the far-jet region. No velocity-profile data in the near-jet region could be found with which to compare the data of figure 6. The only information found on mean velocity in the near-jet region was the variation of $U_0$ with distance by Crow and Champagne (ref. 2). The present measurements agree with those of reference 2 (fig. 7). The extent of the potential flow core is shown by the region for which $U_0$ is constant ($x/D \lesssim 4$). For $x/D \gtrsim 4$, the velocity drops rapidly, and appears to approach an exponential variation far downstream.

## Fluctuating Flow Measurements

The velocity fluctuations across the jet are plotted in the nondimensional form in figures 8-10. As was explained with respect to the mean-flow velocities, various values of $\delta$ were also used to normalize the distance in the analysis of fluctuating velocities. The results were consistent with those described for the mean velocities, thus the only data presented are those where $\delta$ was taken at $0.1U_o$.

The fluctuating velocities do not exhibit similarity as was observed in the case of the mean velocities. This is most notable in the central core of the jet (i.e., for $y/\delta \lesssim 0.5$). In contrast to the central core, the outer half of the jet appears to be approaching similarity more rapidly. The general shape of the crossflow distribution of $\tilde{u}$ is much like that of $\tilde{v}$. The primary difference is that $\tilde{u}$ is always larger than $\tilde{v}$ at a given point in the flow. For both quantities, the crossflow distributions change most rapidly near the jet (from $x/D$ of 3.3 to 6.7); thereafter, changes occur more slowly with distance away from the nozzle. Proceeding downstream, the quantities $\tilde{u}/U_o$, $\tilde{v}/U_o$, and $\overline{u'v'}/U_o^2$ generally increase. The peak values of these quantities (fig. 11) exhibit a near-linear variation with distance. The values of $(\tilde{u}/U_o)_{max}$ are about 50% greater than $(\tilde{v}/U_o)_{max}$. The nonsimilar fluctuating velocities suggest that turbulence has not yet reached the equilibrium or fully developed condition. This result is consistent with the results of Wygnanski and Fiedler (ref. 6), which show that fully developed turbulence is not achieved until $x/D > 50$.

## Four Quadrants of Reynolds Stress

Measurements of the four quadrants of Reynolds stress have previously been restricted to wall shear flows (refs. 7 and 8). In these flows, the $\overline{u'_+v'_-}$ and the $\overline{u'_-v'_+}$ components provide the main contribution to the shear stress ($u'_+$ downstream, $v'_+$ away from the wall). Turbulence was found to be most active during certain phases of the flow; this was true especially near the wall. The main events in the stress-producing process are termed ejection and sweep. During ejection, fluid elements are pushed away from the wall towards the outer flow ($\overline{u'_-v'_+}$) in an impulsive manner and the void thus created by the removal of fluid is filled by the outer flow sweeping towards the wall ($\overline{u'_+v'_-}$). These two events occur in a sequential manner with a time lag and they form a part of the recycling process that joins the inner and outer flows in a boundary layer.

In the present experiments, the four quadrants of the Reynolds stress ($\overline{u'_+v'_+}$, $\overline{u'_-v'_-}$, $\overline{u'_-v'_+}$, $\overline{u'_+v'_-}$) were determined across the jet at $x/D$ of 6.7 and 11.9 (fig. 12). The measured values of $u'$ and $v'$ were put into a half-wave rectifier to separate the positive and negative components of the wave. These components were combined in a multiplier circuit (see fig. 2). For this jet flow, the contribution to the total $\overline{u'v'}$ is mainly from $\overline{u'_+v'_+}$, but the contribution from $\overline{u'_-v'_-}$ is significant. At $x/D$ of 6.7, the value of $\overline{u'_+v'_+}$ is about 100% greater than $\overline{u'_-v'_-}$ over the entire jet thickness. At $x/D$ of 11.9, $\overline{u'_+v'_+}$ and $\overline{u'_-v'_-}$ are nearly the same on the jet centerline, but $\overline{u'_+v'_+}$

4

remains the dominant quantity at the outer edge of the jet while $\overline{u'_-v'_-}$ goes nearly to zero. The $\overline{u'_+v'_+}$ component in the jet is produced by the flow moving away from the centerline at a positive angle in the direction of the spread, whereas $\overline{u'_-v'_-}$ is a result of the inward flow towards the nozzle. Production of shear is thus stronger in the outward rather than the inward flow.

In some respects, one half of the jet can be considered as a boundary layer with the wall removed (i.e., the free-stream velocity on the centerline and the wall at the outer edge of the jet). Because the sign convention for the jet has been $v'_+$ toward the outer edge of the jet (which is opposite to the boundary layer convention), the sign of $v'$ must be changed for this consideration. The values of $\overline{u'_+v'_+}$ and $\overline{u'_-v'_-}$, which were found to provide the major contribution to $\overline{u'v'}$ in the jet, will now be $\overline{u'_+v'_-}$ and $\overline{u'_-v'_+}$. These are the same quantities found most important in the boundary-layer flows. These main activities in the jet flow suggest the possibility of a large turbulent recirculating flow somewhat similar to the pattern observed by others in a boundary layer.

## Large-Scale Velocity Fluctuations

Large-scale velocity fluctuations are important to understanding the structure of turbulence because they contain most of the total kinetic energy. In general, the structure of a turbulent flow consists of a variety of scales from small to large. An examination of the $u'$ or $v'$ signals (samples shown in fig. 13) suggests that the large-scale (low-frequency) fluctuations are the carrier waves with the small-scale (higher-frequency) fluctuations superimposed on them. Filtering can be used to separate the high-frequency signals from the low-frequency signals, but there is uncertainty in the selection of the cutoff frequency. In our investigation, the large-scale fluctuations were identified directly from the $u'$ and $v'$ traces by fairing a curve through the trace to eliminate the small-scale, high-frequency fluctuations and to emphasize the large-scale excursions (fig. 13). The number of large-scale fluctuations in a given trace were estimated by counting the zero crossings of these large-scale signals. As with filtering, this method also involves uncertainty; for some portions of the trace, judgment becomes significant. There seems to be no exact way to make this analysis.

The large-scale fluctuations (zero crossings) were estimated across the jet at $x/D$ of 6.7 and 11.9 for the $u'$ traces. The rate of zero crossings $(N_c)$ over the width of the jet varied appreciably (fig. 14). However, a Strouhal number based on the local mean velocity $(U)$, the nozzle diameter $(D)$, and the frequency of zero crossings $(f)$, was found to have a relatively constant value with the exception of a few widely scattered points at the outer edge of the jet (fig. 15). The Strouhal number was about $0.22 \pm 0.05$.

The variation in the rate of occurrence of the large-scale structures across the jet (as indicated by $N_c$) suggests that the total jet involves more than one turbulence scale, in contrast to the boundary layer, where a single eddy structure predominates (ref. 9). The near-jet region probably contains several turbulence scales; one scale might originate in the core flow of the

jet and the other from the induced outer flow. As the flow moves downstream, the distinction between the two scales would probably vanish and a single, large scale would result. Such a trend might be deduced from the zero crossings of the u' fluctuations (fig. 14).

It has not been clear from existing research whether Reynolds stress is the result of small-scale motions or large-scale motions. The u'v' trace (fig. 13) shows large, conspicuous, positive amplitude signals that appear at a random time interval of $T_{u'v'}$. Several of the positive spikes have been crosshatched for reference. These signals persist for a time t that is small relative to $T_{u'v'}$. These signals impart an appearance of intermittency to the trace. In contrast to the large, positive disturbances, the smaller disturbances are more symmetrically distributed around the mean. The contribution of these smaller disturbances to the total $\overline{u'v'}$ might, therefore, be considered negligible. Thus the large, positive fluctuations that persist for time t appear to form the shear stress; this result is consistent with the measurements of the four quadrants of $\overline{u'v'}$ (i.e., the positive u'v' peaks are produced by both $\overline{u'v'}_+$ and $\overline{u'v'}_-$). Because the time scale for this Reynolds stress production (t) is small relative to that for the large-scale structure determined from the zero crossings of u' ($T_{u'}$), it appears that Reynolds stress could be considered a small-scale rather than a large-scale motion.


Periodic Disturbances

The low-speed flow from a jet passes through several defined stages during transition to a fully developed turbulent flow. Initially, instability develops in the shear layer at the nozzle exit. This initial, small-scale instability increases to a large-amplitude oscillation that is associated with vortex formation. As the vortices develop, adjacent ones interact and pair with each other. The jet becomes turbulent following the pairing process. Further detailed discussion of this transition in a jet can be found in reference 5.

Experiments of the transitory flow near the nozzle exit were run at three velocities ($U_e$ of 9, 29 and 54.6 m/sec). To observe the development of the flow instability, a single, normal hot wire was used at various x stations along the jet centerline. The resulting hot-wire traces are a measure of u' as a function of time. A set of such u' traces are shown in figure 16 for the value of $U_e$ = 29 m/sec (the transition region is compressed at higher velocity and stretched out at lower velocity).

The formation of the instability patterns at the onset of transition, as well as the vortex pairing, could be identified from the hot-wire traces (e.g., refer to fig. 16). The fluctuations were small for x/D ⩽ 0.5, but were rapidly amplified and exhibited a well-defined periodicity. During this amplification process, the fluctuations appear to be amplitude modulated. At x/D of about 2, the frequency became half of the original value; this represented the pairing process. No further pairing was observed. The formation of random turbulent fluctuations was always observed downstream of pairing

(x/D $\gtrsim$ 2 for $U_e$ = 29 m/sec, fig. 16). This apparently represents the development of a fully turbulent jet. The frequency of the oscillations were counted from the traces. During the amplification of the initial instability (prior to pairing), the Strouhal number was about $0.7^{\pm 0.1}$ (e.g., at $U_e$ of 29 m/sec, this frequency would be determined in the region of $0.5 \lesssim x/D < 1.0$). At pairing (x/D ~ 2 for $U_e$ = 29 m/sec), the Strouhal number was about $0.35^{\pm 0.05}$, a value close to 0.3, a value that some investigators have found to be significant in the far-field studies of jets (e.g., ref. 2).

In the present experiments, vortex pairing appears to be the completion of the instability process that precedes the fully developed turbulent jet. Because the measurements described in the previous paragraph showed that the length of this region varied with $U_e$, measurements were made to define this variation. A single, normal hot wire was fixed on the jet centerline at arbitrarily selected x stations. To indicate that pairing was completed, $U_e$ was varied until the desired trace was observed (e.g., like that at x/D = 1.97 in contrast to those at x/D = 1.57 and 2.36, fig. 16). The resulting data are shown in figure 17. Pairing was not observed below $U_e$ of 9 m/sec ($R_D$ ~ 7500). At the high velocity end of the curve, it appears that pairing approaches the nozzle exit asymptotically.

## CONCLUSIONS

The near region of an axisymmetric jet was investigated for the large-scale turbulent fluctuations. The mean-velocity profiles and the turbulent-velocity fluctuations (u', v', and u'v') were measured. Similarity was observed in the mean-velocity profiles for x/D $\gtrsim$ 6, whereas the nondimensionalized turbulence velocities varied over the entire region investigated. Although the large-scale structure (represented by zero crossings) varied across the jet, a Strouhal number based on frequency of occurrence of these large-scale fluctuations was relatively constant.

An analysis of the four quadrants of Reynolds stress and an analysis of the u'v' trace indicated that the same quadrants that are significant to the total Reynolds stress in boundary-layer flow are also most important in the jet flow. Further, it appears that Reynolds stress might result from small-scale rather than large-scale motion.

Initial instability waves and vortex pairing occurred at a Strouhal number of 0.7 and 0.35, respectively. The jet became turbulent only downstream of the vortex pairing.

# REFERENCES

1. Fuchs, H. V.: Space Correlation of the Fluctuating Pressure in Subsonic Turbulent Jets. Journal of Sound and Vibration, 2 (1), 1972, pp. 77-99.

2. Crowe, S. C.; and Champagne, F. M.: Orderly Structure in Jet Turbulence. J. Fluid Mech., vol. 48, 1971, pp. 547-592.

3. Mollo-Christensen, E.; and Narasimha, R.: Sound Emission from Jets at High Subsonic Velocities. J. Fluid Mech., vol. 8, 1960, pp. 49-60.

4. Fuchs, H. V.; and Armstrong, R. R.: Turbulence Source Coherence and Helmholtz Number as Aerodynamic Noise Parameters. Conference Proceedings, Symposium on Turbulence, Aug. 1-5, 1977, Berlin.

5. Laufer, J.; Kaplan, R. E.; and Chu, W. T.: On the Generation of Jet Noise. AGARD Conference Proceedings, CP No. 131 — Noise Mechanisms, 1974.

6. Wygnanski, I.; and Fiedler, H.: Some Measurements in the Self Preserving Jet. J. Fluid Mech., vol. 38, 1969, pp. 577-612.

7. Wallace, J. M.; Eckelmann, H.; and Brodkey, R. S.: The Wall Region in Turbulent Shear Flow. J. Fluid Mech., vol. 54, 1972, pp. 39-48.

8. Badri Narayanan, M. A.; Rajagopalan, S.; and Narasimha, R.: Experiments on the Fine Structure of Turbulence. J. Fluid Mech., vol. 80, 2, 1977, pp. 237-257.

9. Badri Narayanan, M. A.; and Marvin, J. C.: On the Period of the Coherent Structure in Boundary Layers at Large Reynolds Number. NASA TM 78,477, 1978.
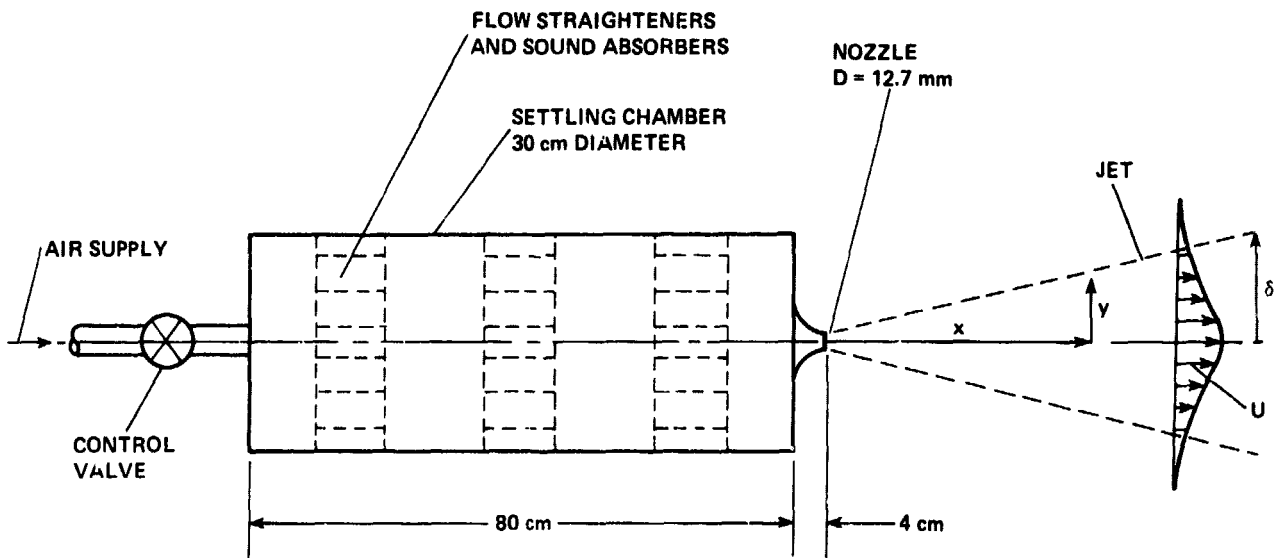
Figure 1.- Axisymmetric jet.

9
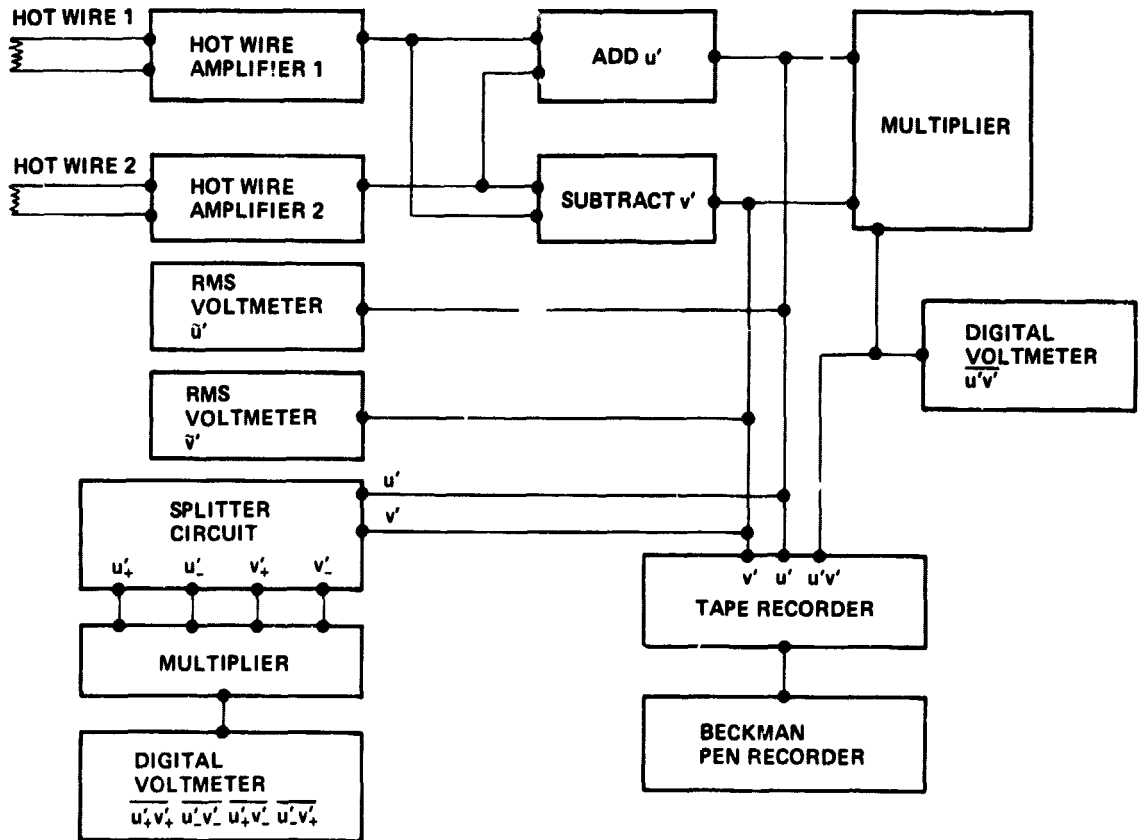
Figure 2.- Signal processing.

10

| | x/D | $U_0$, m/sec | $\delta$, mm AT 0.05 $U_0$ | $\delta$, mm AT 0.10 $U_0$ |
|---|---|---|---|---|
| O | 3.3 | 54.6 | 17.5 | 13.8 |
| □ | 6.7 | 48.5 | 37.5 | 22.0 |
| ◇ | 11.9 | 29.7 | 42.0 | 32.5 |
| △ | 22.8 | 16.0 | 95.0 | 75.0 |
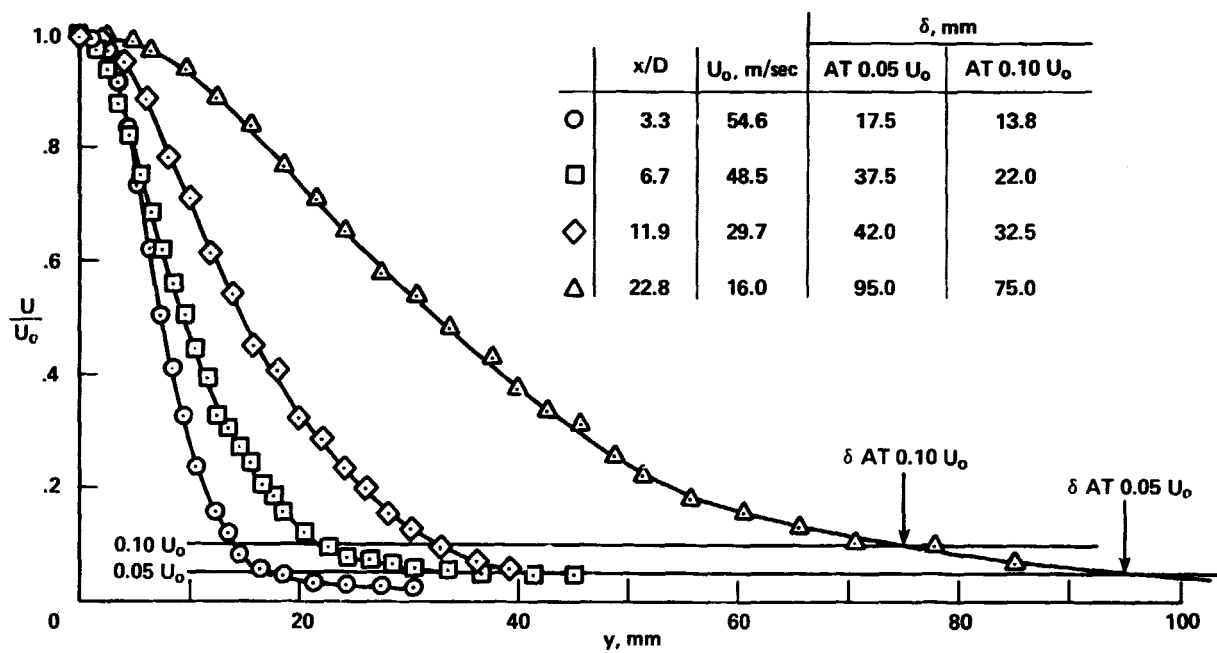
Figure 3.- Mean-flow velocity across the jet.
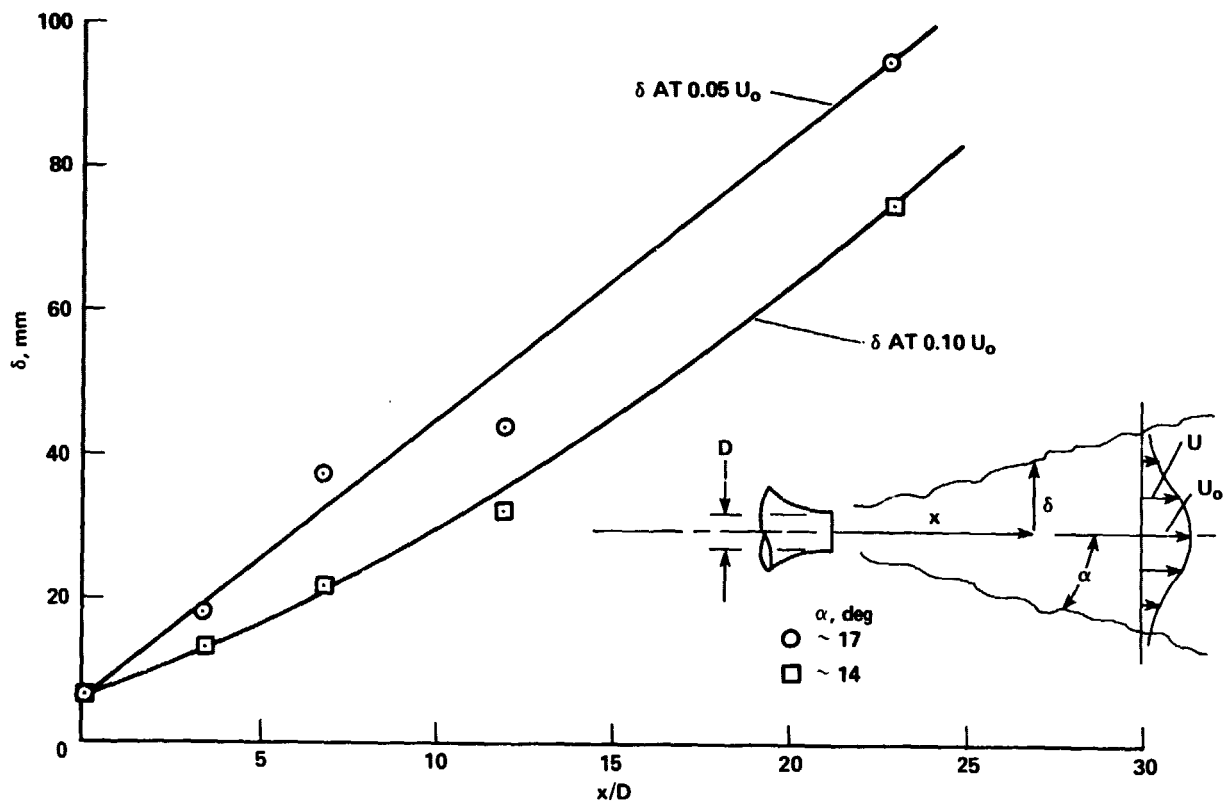
Figure 4.- Jet thickness, $\delta$.
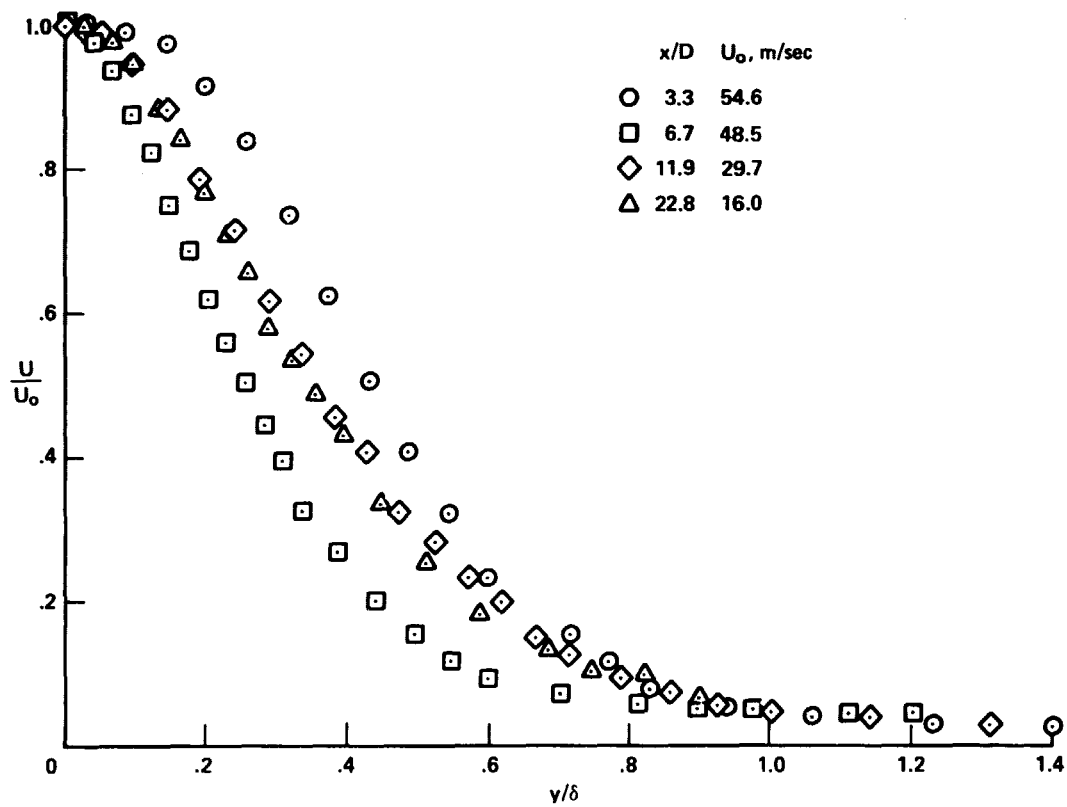
Figure 5.- Nondimensionalized mean-flow velocity profiles; $\delta$ determined at $0.05U_o$.
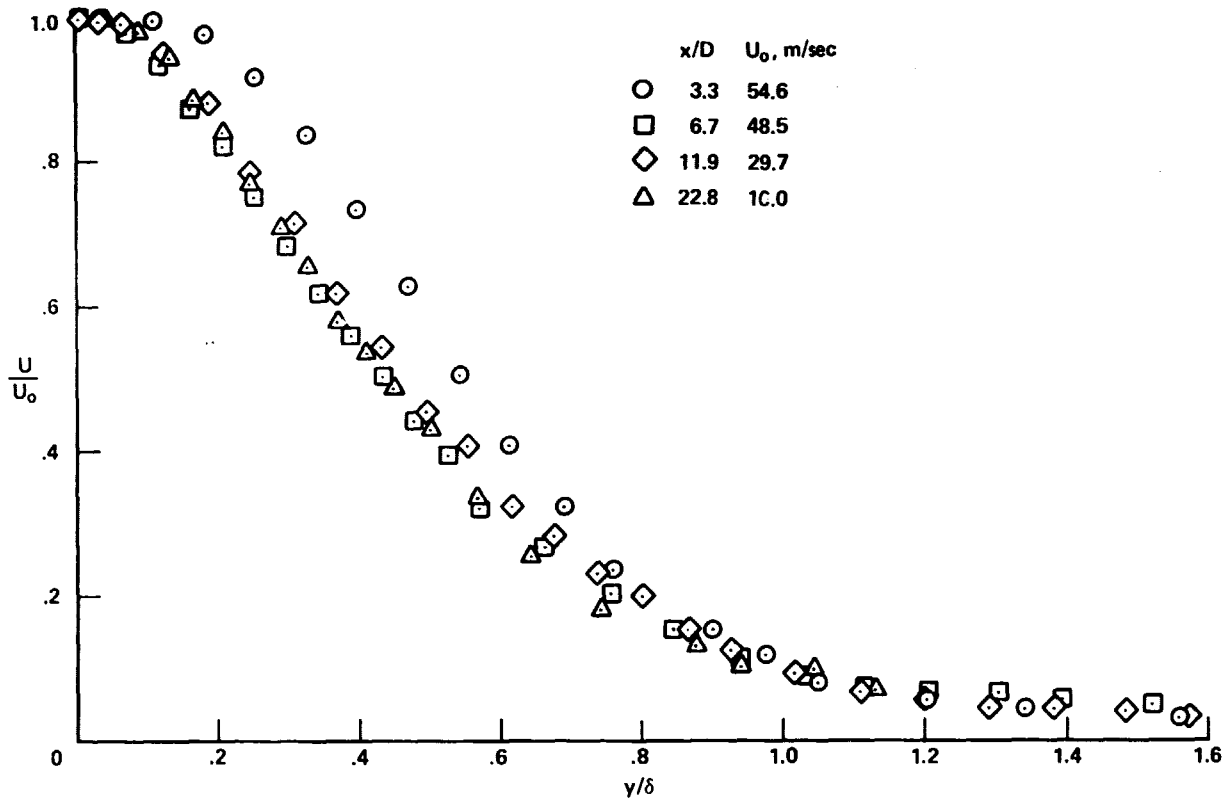
Figure 6.- Nondimensionalized mean-flow velocity profiles; $\delta$ determined at $0.10U_0$.
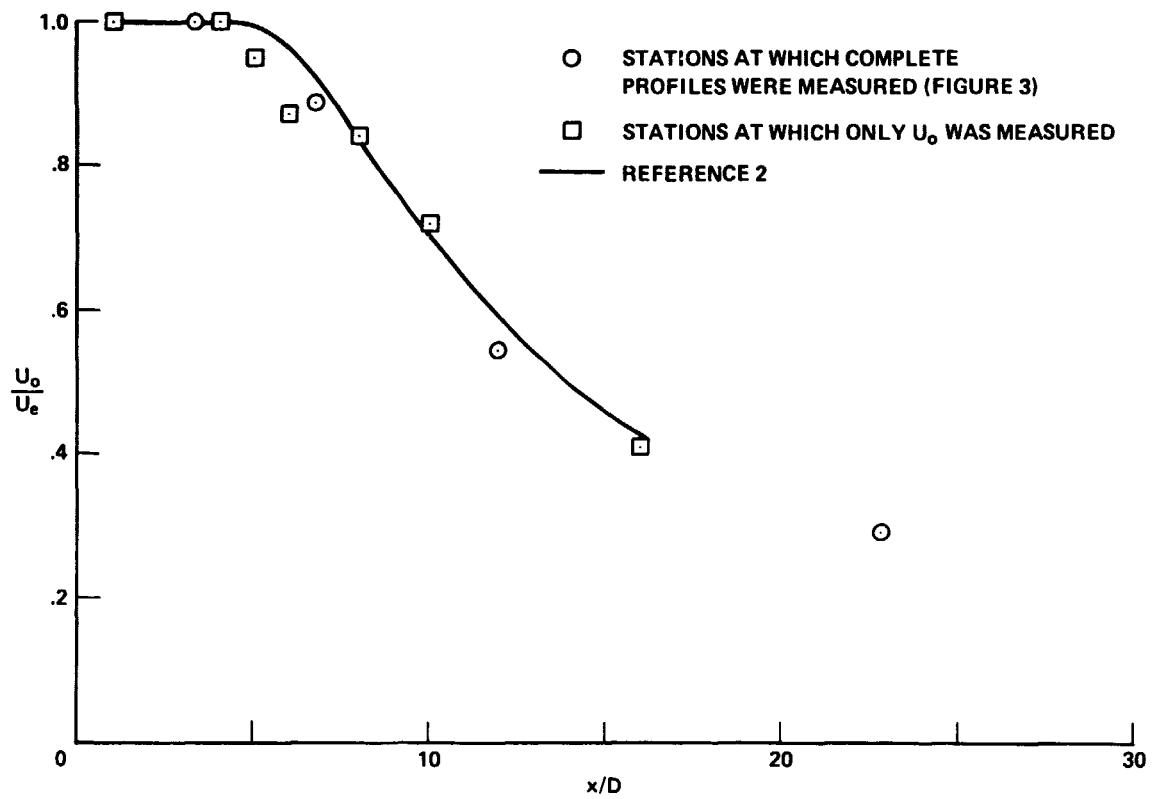
Figure 7.- Variation of mean velocity along the jet axis.

15
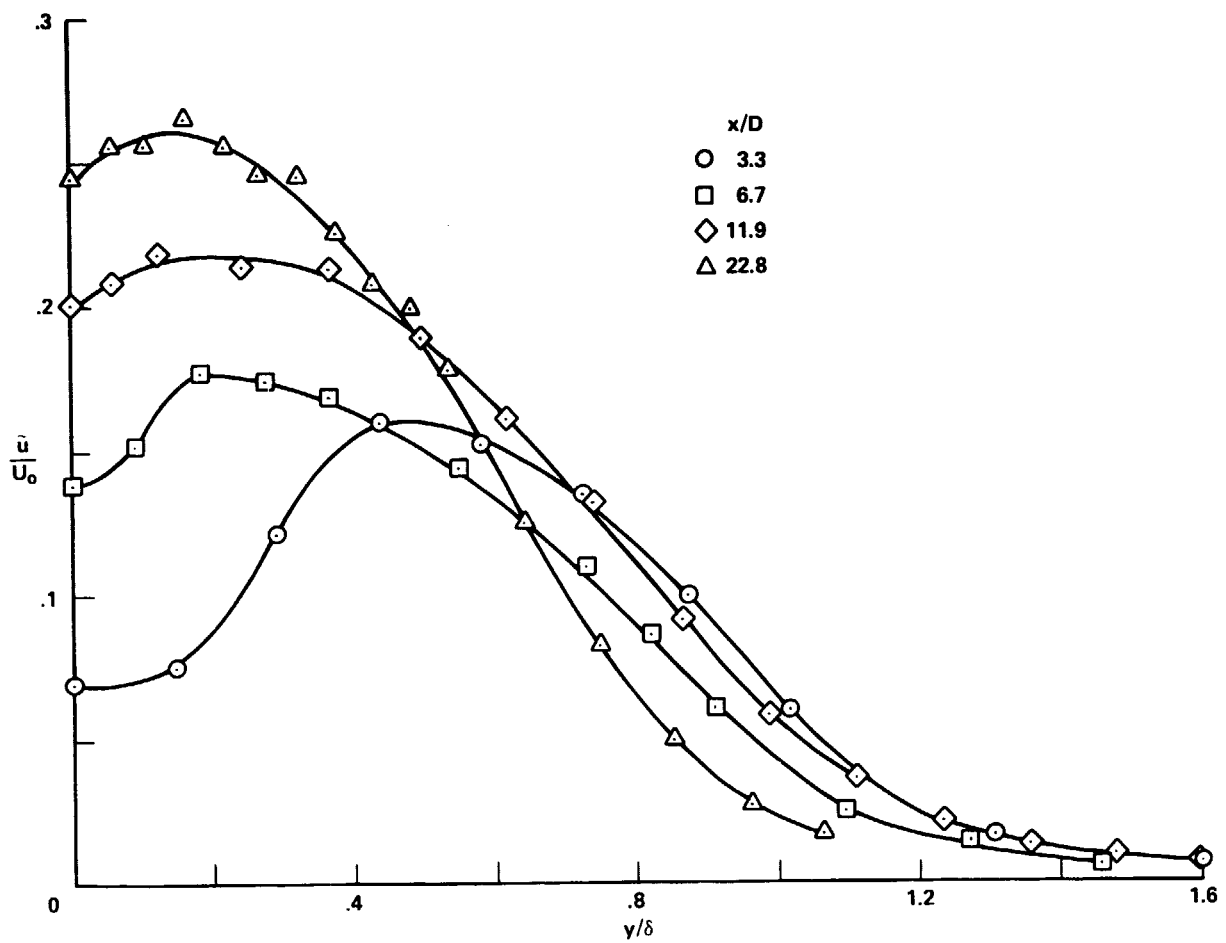
Figure 8.- Distribution of u'  across the jet.
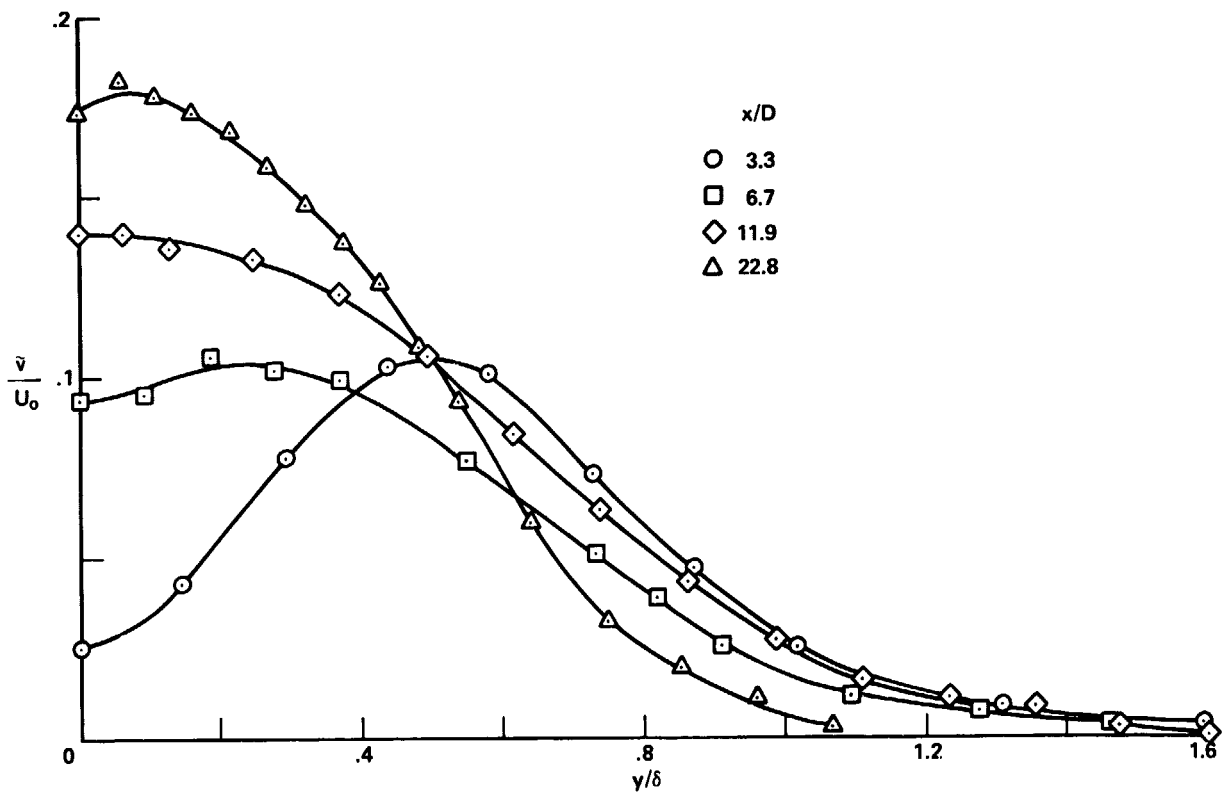
Figure 9.- Distribution of v' across the jet.

17
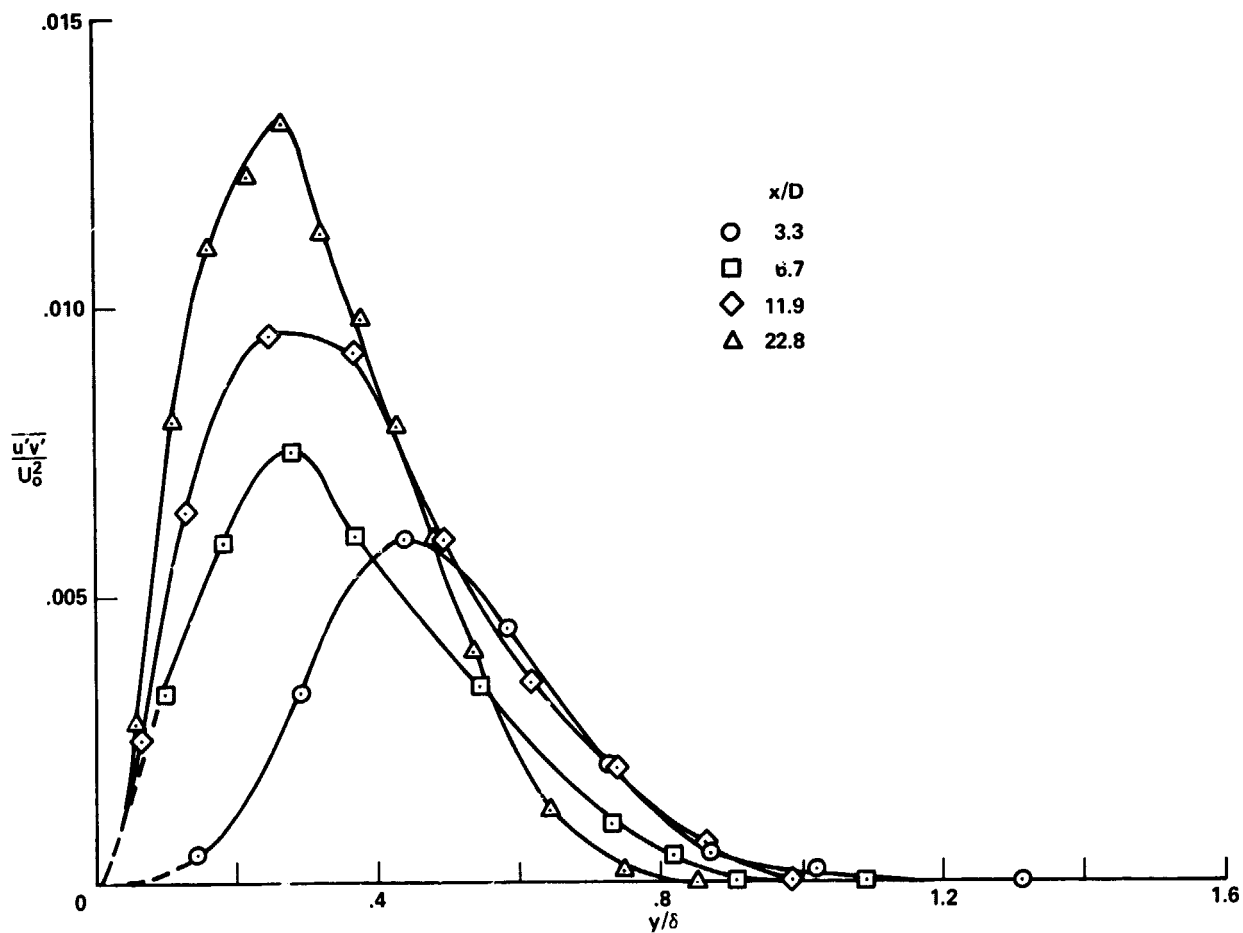
Figure 10.- Distribution of $\overline{u'v'}$ across the jet.
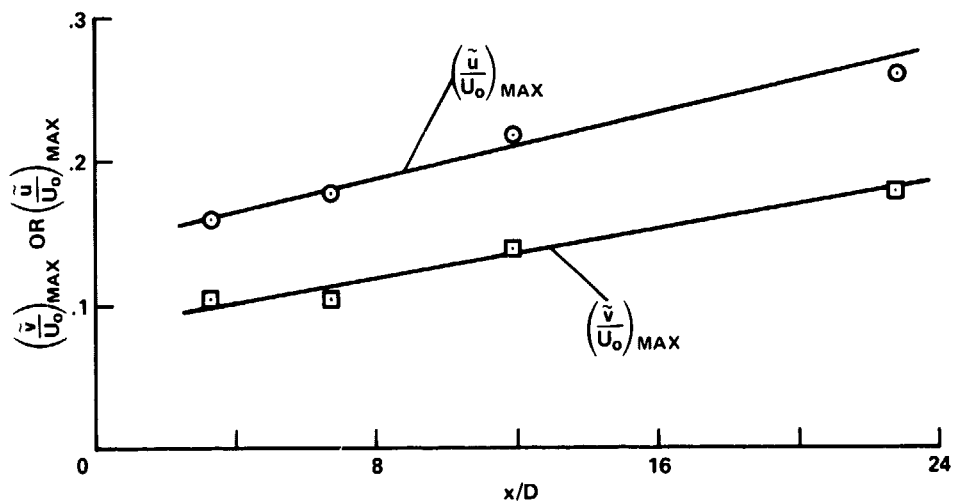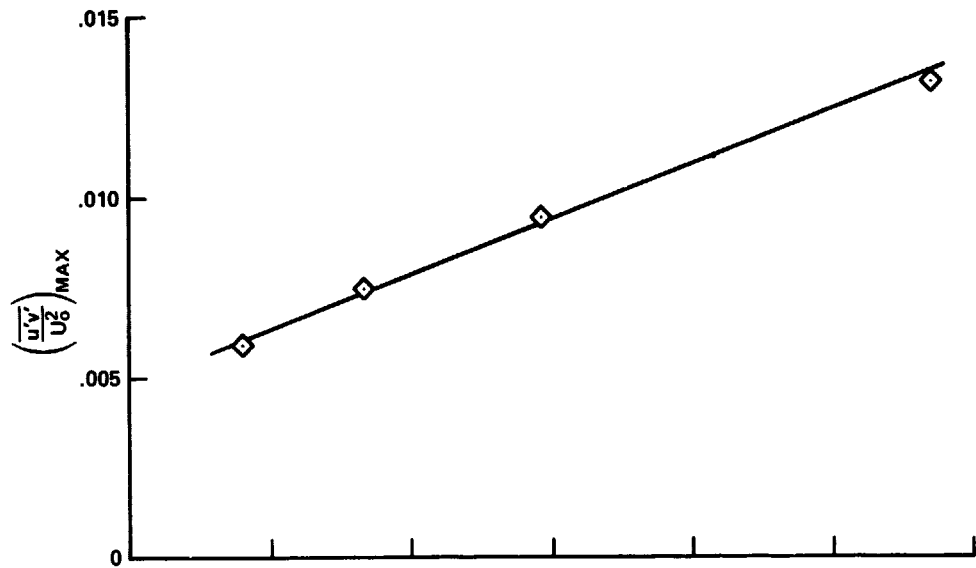
Figure 11.- Variation of the maximum values of  ũ, ṽ and $\overline{u'v'}$.

19
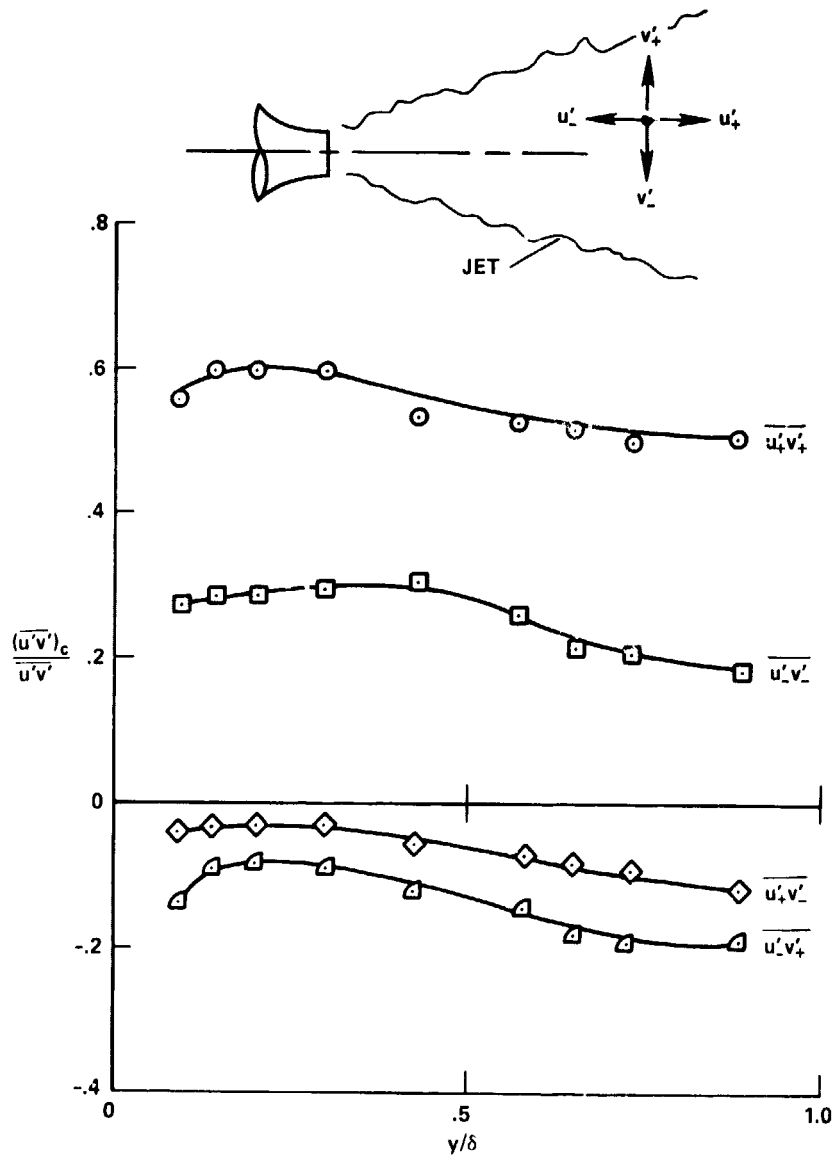
a) x/D = 6.7

Figure 12.- Components of $\overline{u'v'}$.

20
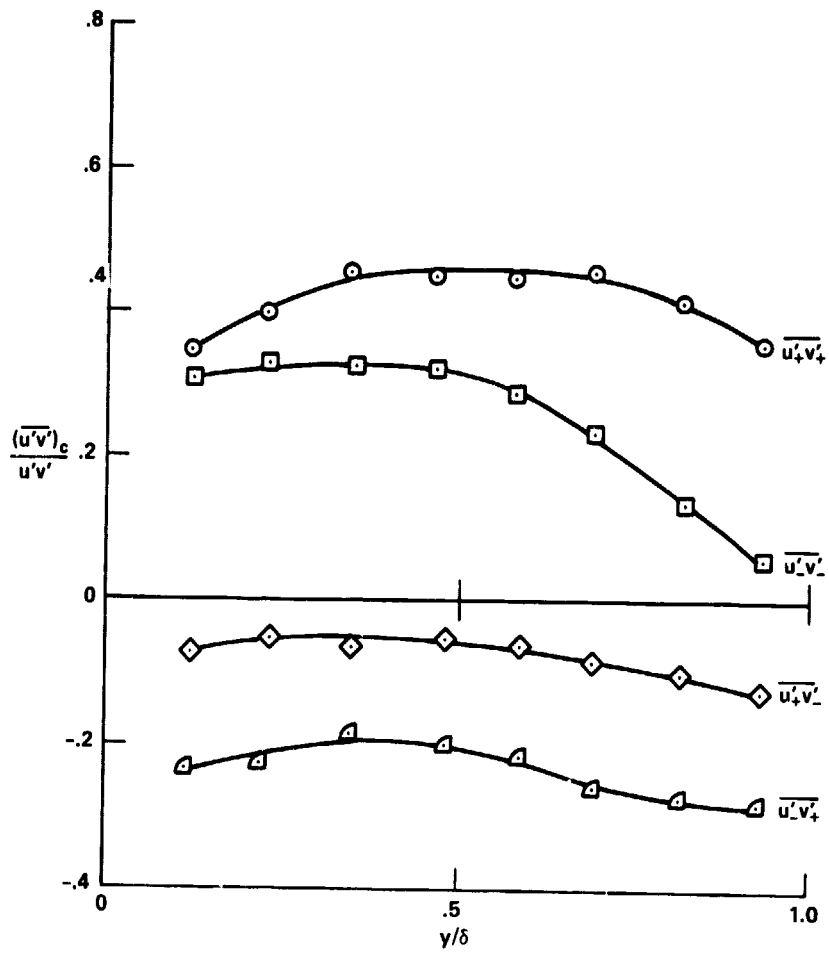
b) $x/D = 11.9$

Figure 12.- Concluded.

21
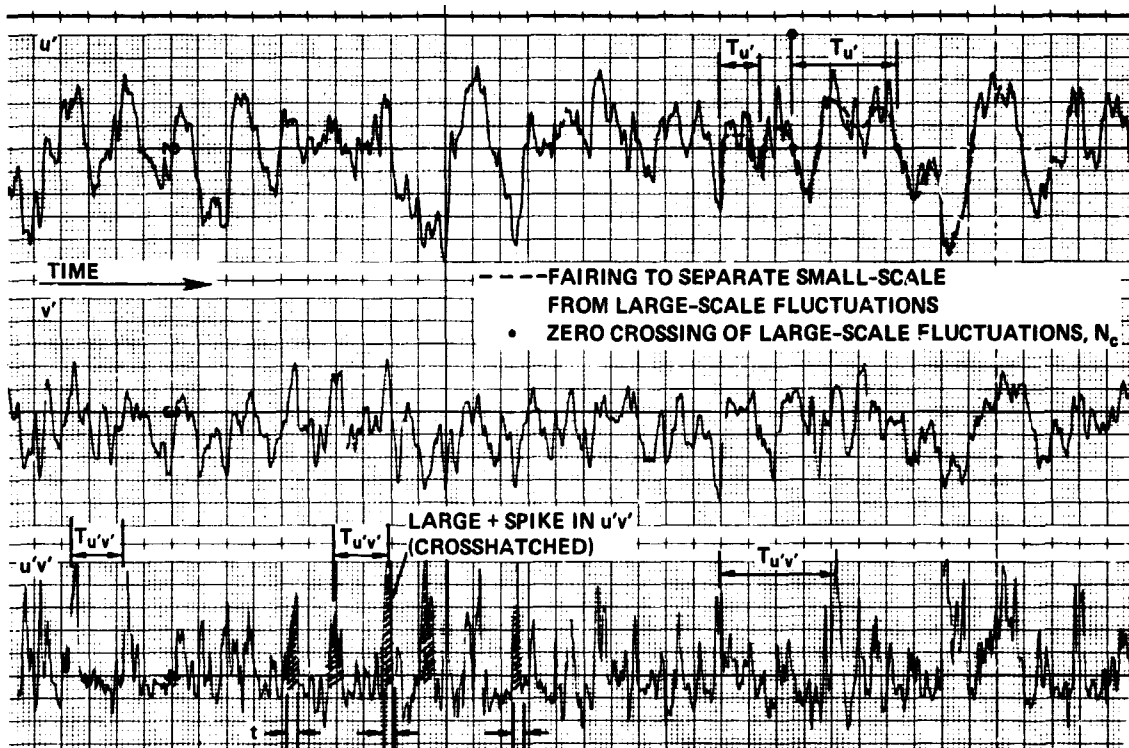
Figure 13.- Simultaneous records of  u', v' and u'v'.
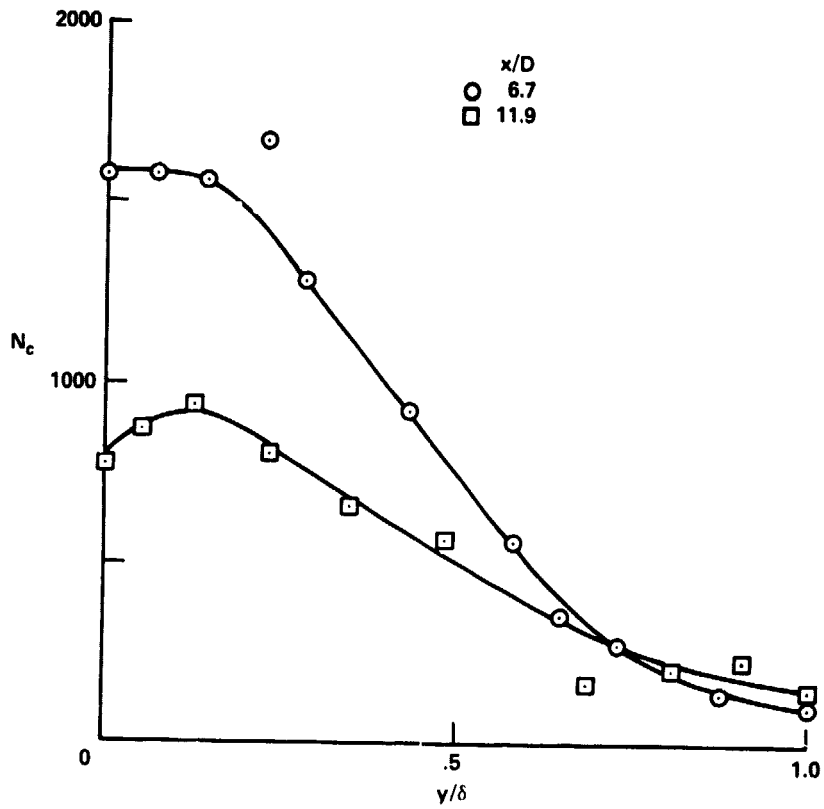
Figure 14.- Rate of large-scale zero crossings for u'.
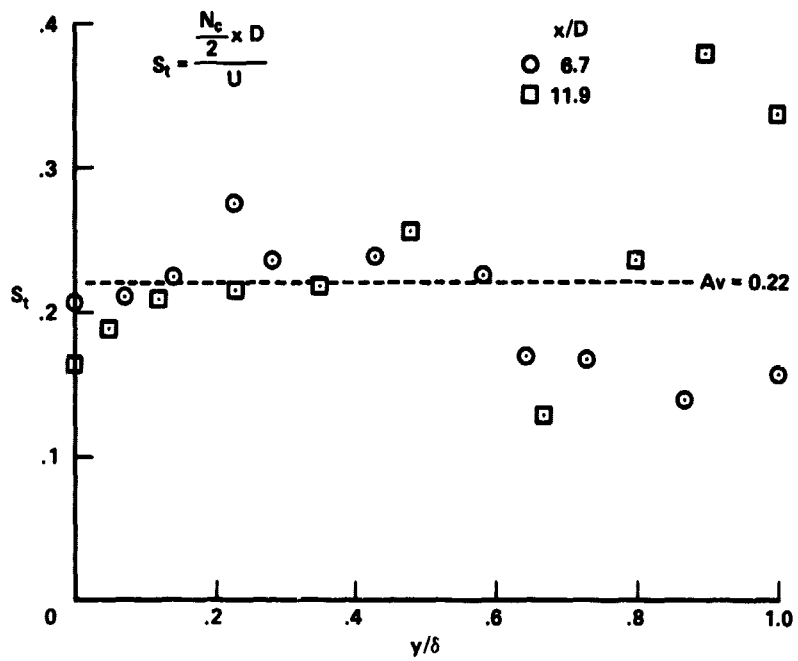
Figure 15.- Strouhal number for the u' zero-crossing data.
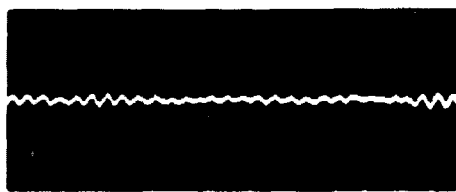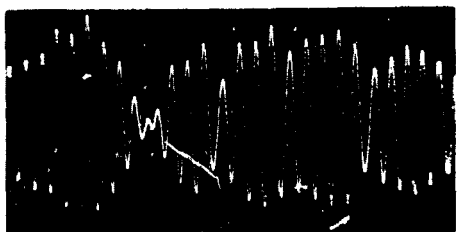
(a) x/D = 0
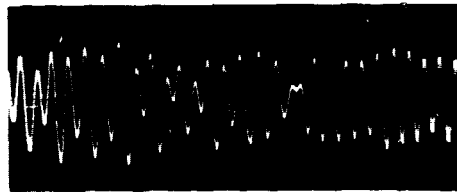
(b) x/D = 0.39

(c) x/D = 0.79

(d) x/D = 1.18
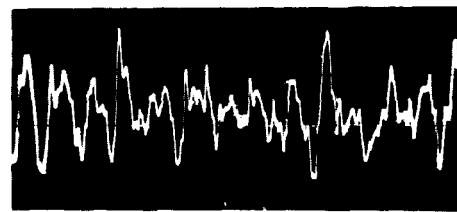
(e) x/D = 1.57
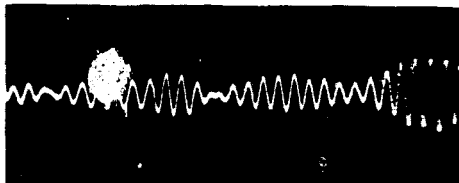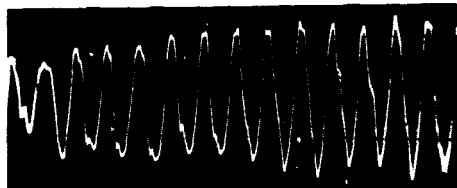
(f) x/D = 1.97
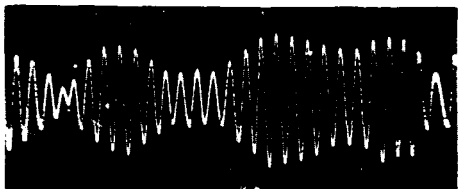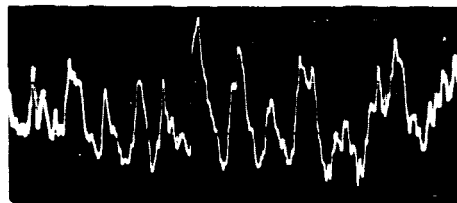
(g) x/D = 2.36

(h) x/D = 2.76

Figure 16.- Oscilloscope traces of  u'  fluctuations using a single, normal
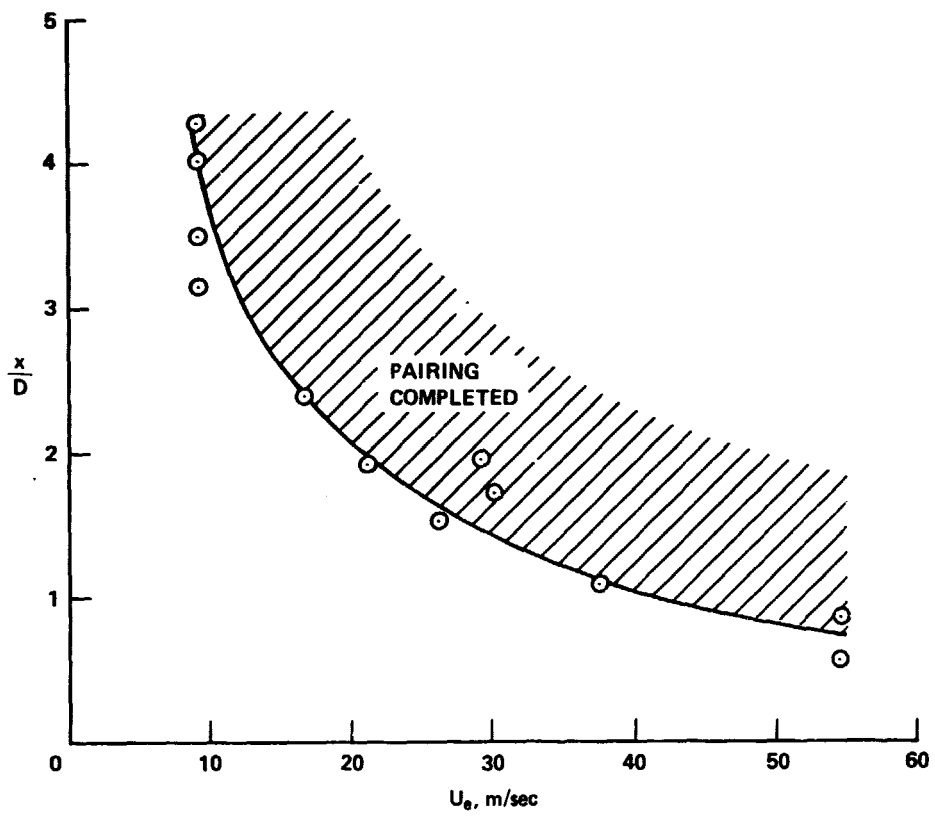hot wire on the centerline of the jet; $U_e$ = 29 m/sec.

Figure 17.- Station at which the vortex pairing is completed.

26